Electronic Supplementary Information

Experimental probing of dynamic self-organized columnar assemblies in colloidal liquid crystals

Taiki Hoshino[a,b,c*†], Masanari Nakayama[d*†], Yoshihiro Hosokawa[d], Kohei Mochizuki[d], Satoshi Kajiyama[d], Yoshiki Kohmura[b], Takashi Kato[d,e*]

[a] International Center for Synchrotron Radiation Innovation Smart (SRIS), Tohoku University, 2-1-1 Katahira, Aoba-ku, Sendai 980-8577, Japan

[b] RIKEN SPring-8 Center, 1-1-1, Kouto, Sayo-cho, Sayo-gun, Hyogo 679-5148, Japan

[c] Institute of Multidisciplinary Research for Advanced Materials (IMRAM), Tohoku University, 2-1-1 Katahira, Aoba-ku, Sendai 980-8577, Japan

[d] Department of Chemistry and Biotechnology, School of Engineering, The University of Tokyo, Tokyo 113-8656, Japan

[e] Research Initiative for Supra-Materials, Shinshu University, 4-17-1, Wakasato, Nagano, Japan

† Equal Contribution

*Taiki Hoshino

Email: taiki.hoshino.c7@tohoku.ac.jp

*Masanari Nakayama

Email: masanarinakayama@gmail.com

*Takashi Kato

Email: kato@chiral.t.u-tokyo.ac.jp

Contents

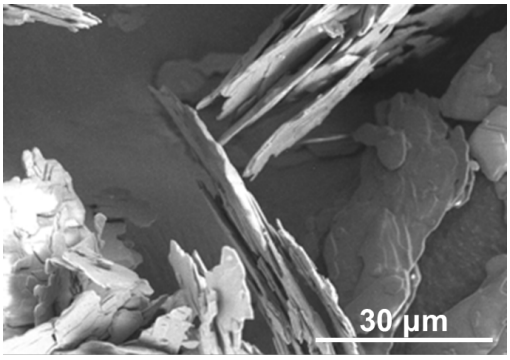

Fig. S1. Scanning electron microscopy (SEM) image of two-dimensional (2D) templates prepared in the presence of 0.14 wt% poly(acrylic acid) (PAA).

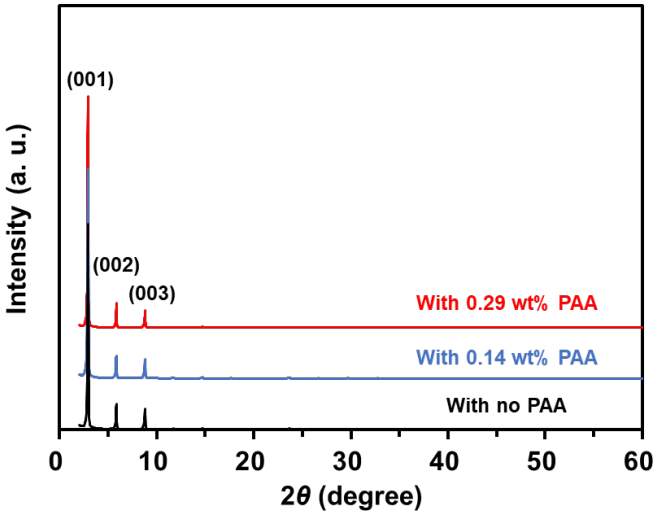

Fig. S2. X-ray diffraction (XRD) patterns of 2D templates prepared in the presence of different PAA concentrations of 0 wt%, 0.14 wt% and 0.29 wt%.

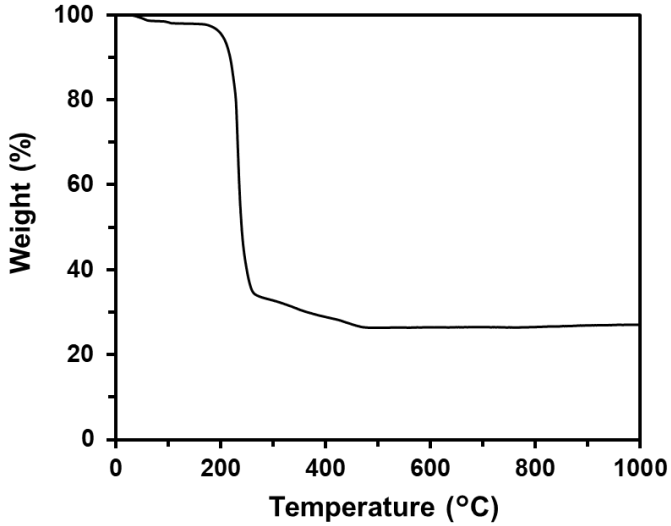

Fig. S3. Thermogravimetric (TG) curve of the 2D templates prepared in the presence of 0.14 wt% PAA.

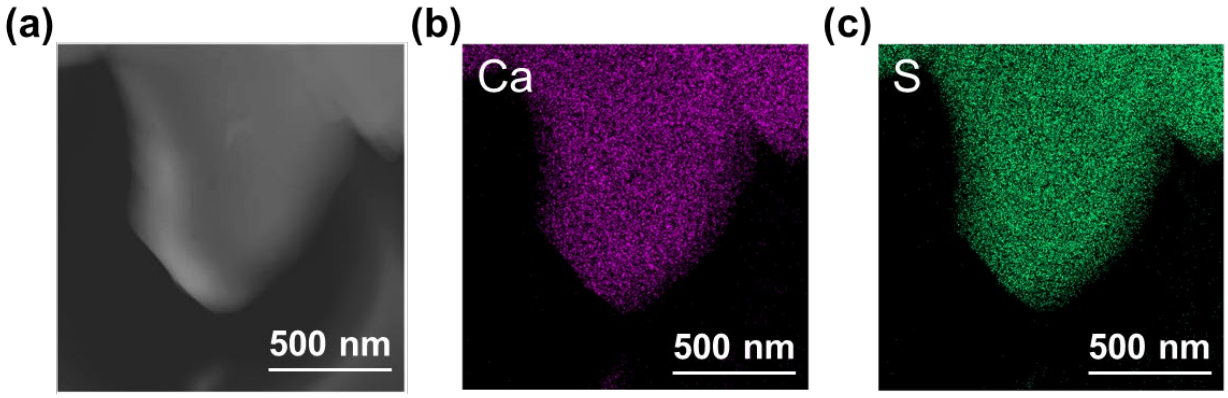

Fig. S4. (a) Transmission electron microscopy (TEM) image of a 2D template prepared in the presence of 0.14 wt% PAA and (b,c) the corresponding energy-dispersive X-ray spectroscopy (EDS) elemental mapping images of (b) Ca and (c) S elements.

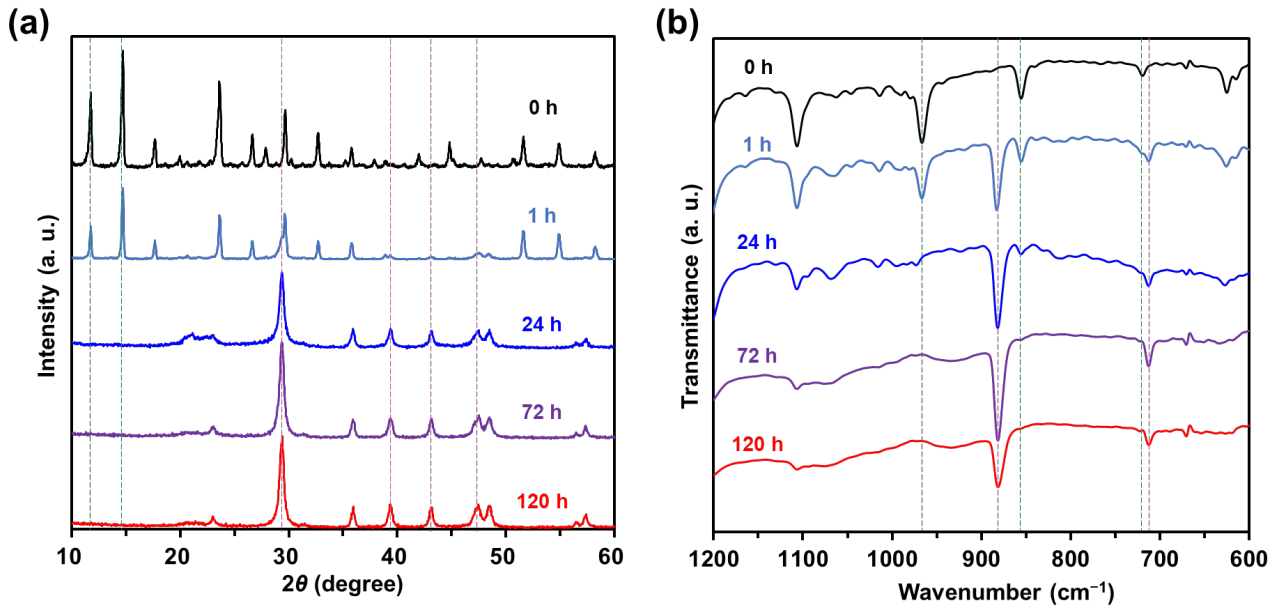

Fig. S5. (a, b) Time-dependent evolutions of (a) XRD patterns and (b) Fourier-transform infrared (FTIR) spectra for precipitates collected at different crystallization times after the addition of Na_2CO_3 into a dispersion of Ca^{2+} layers inside the organic templates. Green and pink dashed lines indicate characteristic peaks for calcium dodecyl sulfonate crystals and calcite crystals, respectively.

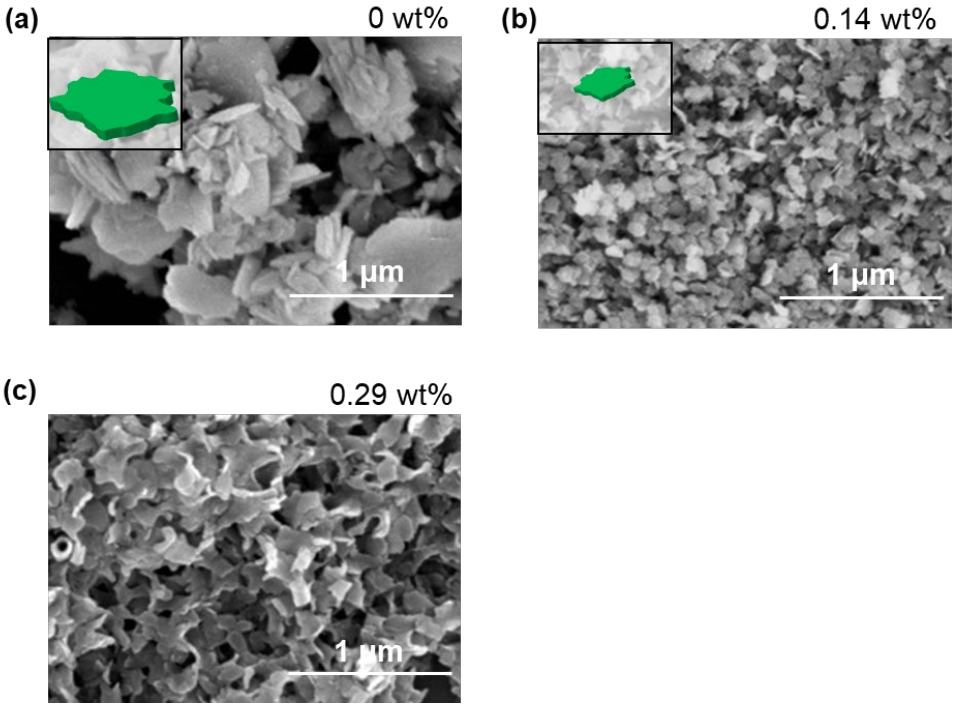

Fig. S6 SEM images of precipitates prepared at different PAA concentrations of (a) 0 wt%, (b) 0.14 wt%, and (c) 0.29 wt% with the corresponding shape illustration in (a) and (b). All the precipitates were obtained at SDS concentration of 80 mM.

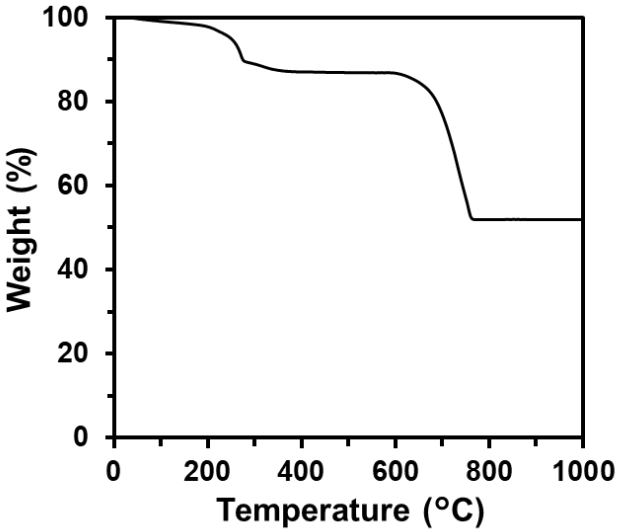

Fig. S7. TG curve of wide-disperse nanoplates after drying.

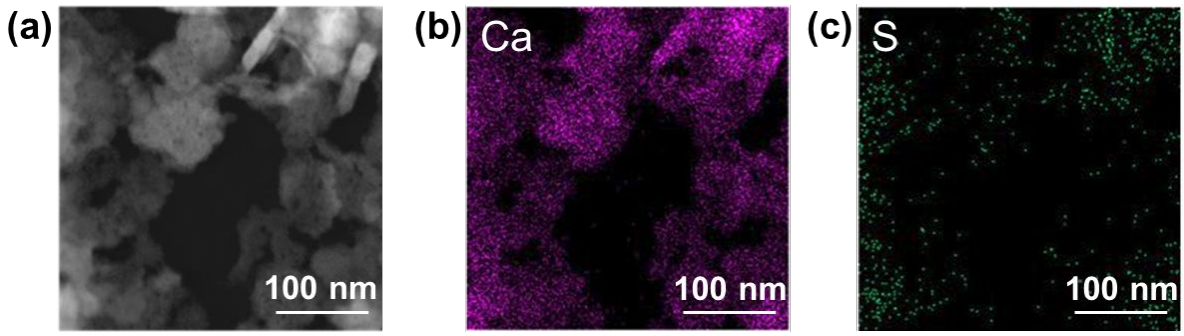

Fig. S8. (a) TEM image of wide-disperse nanoplates and the corresponding EDS elemental mapping images of (b) Ca and (c) S elements.

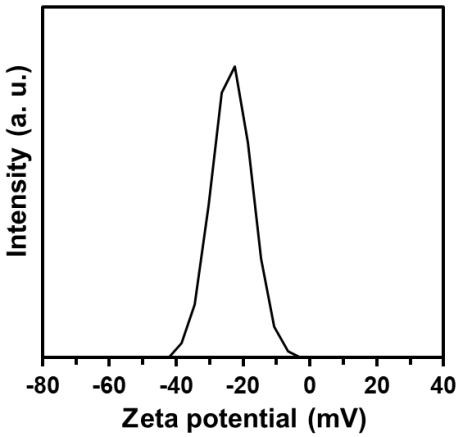

Fig. S9. Zeta potential curve of a colloidal dispersion of wide-disperse nanoplates.

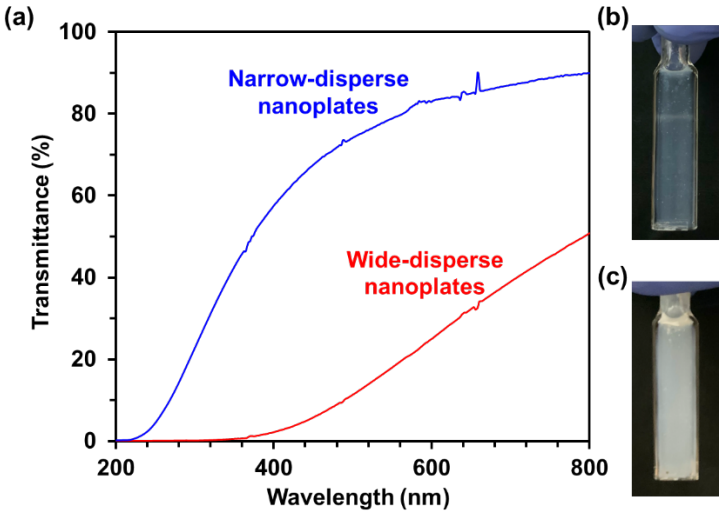

Fig. S10. (a) Transmittance spectra of 19.8 vol% colloidal dispersions of wide-disperse and narrow-disperse nanoplates. (b, c) Photographs of the colloidal dispersions of (b) narrow-disperse and (c) wide-disperse nanoplates.

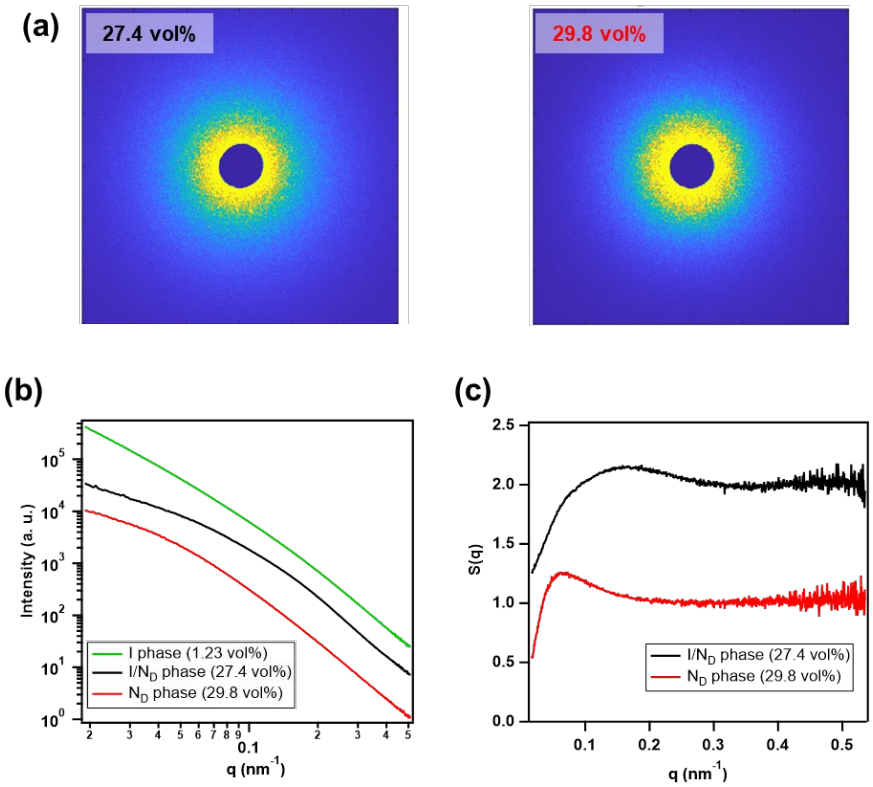

Fig. S11. (a) 2D small-angle X-ray scattering (SAXS) patterns of colloidal dispersions of wide-disperse nanoplates at different concentrations of 27.4 vol% and 29.8 vol%. (b) SAXS profiles of colloidal dispersions of wide-disperse nanoplates at different concentrations of 1.23 vol%, 27.4 vol%, and 29.8 vol%. (c) Structure factors S(q) of colloidal dispersions of wide-disperse nanoplates at different concentrations of 27.4 vol% and 29.8 vol%.

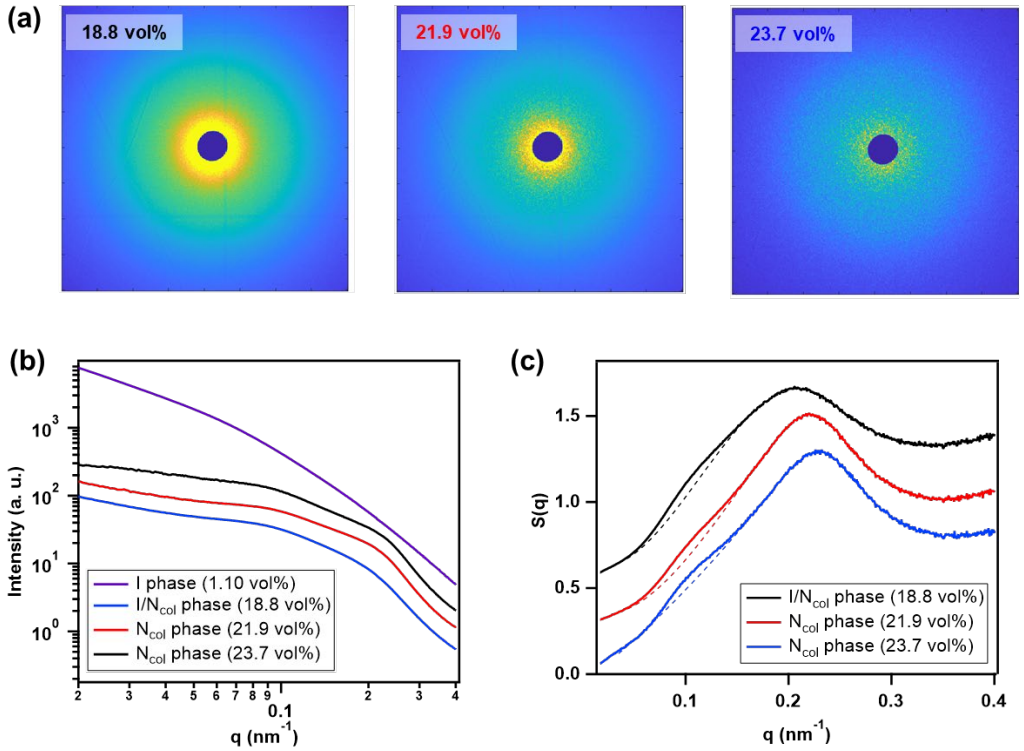

Fig. S12. (a) 2D SAXS patterns of colloidal dispersions of narrow-disperse nanoplates at different concentrations of 18.8 vol%, 21.9 vol% and 23.7 vol%. (b) SAXS patterns of colloidal dispersions of narrow-disperse nanoplates at different concentrations of 1.10 vol%, 18.8 vol%, 21.9 vol% and 23.7 vol%. (c) Structure factors S(q) of colloidal dispersions of narrow-disperse nanoplates at 18.8 vol%, 21.9 vol% and 23.7 vol% with the fitted baselines at around q = 0.1 nm^{-1}.

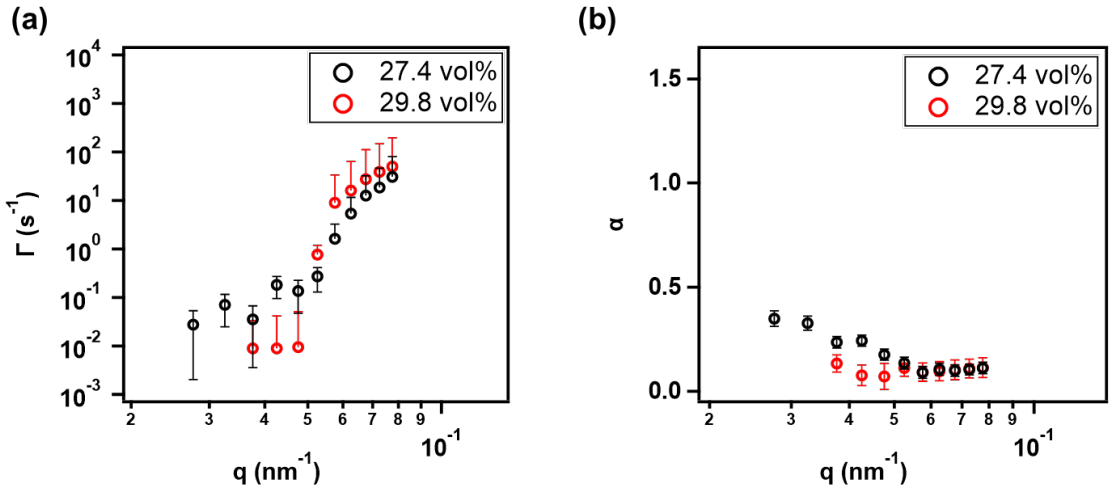

Fig. S13. (a) q dependences of relaxation rates Γ for colloidal dispersions of wide-disperse nanoplates at different concentrations of 27.4 vol% and 29.8 vol%. (b) q dependences of exponents α for colloidal dispersions of wide-disperse nanoplates at 27.4 vol% and 29.8 vol%. Some of the downward error bars are omitted in (a) to avoid complicating the drawing.